의학석사 학위논문

Type I interferon-dependent influenza virus resistance in pulmonary fibrosis model

폐섬유 질환 모델에서 제 1형 인터페론에 의한 인플루엔자 바이러스 저항성

2021년 2월

서울대학교 대학원

의과학과 면역학 전공

정 재 현

A thesis of the degree of Master of Science

폐 섬유 질환 모델에서 제 1형 인터페론에 의한 인플루엔자 바이러스 저항성

Type I interferon-dependent influenza virus resistance in pulmonary fibrosis model

February 2021

Major in Immunology
Department of Biomedical Sciences
Seoul National University

Jae-Hyeon Jeong

Type I interferon-dependent influenza virus resistance in pulmonary fibrosis model

by

Jae-Hyeon Jeong

(Supervised by Prof. Youn Soo Choi)

A thesis submitted to the department of Biomedical Sciences in partial fulfilment of the requirements for the Degree of Master of Science in Medicine (Immunology)
at Seoul National University College of Medicine

February 2021

Approved by Thesis Committee:

February 2021

Chair Doo Hyun Chung (Seal)

Vice Chair Youn Soo Choi (Seal)

Examiner Won-Woo Lee (Seal)

폐 섬유 질환 모델에서 제 1형 인터페론에 의한 인플루엔자 바이러스 저항성

지도교수 최윤수

이 논문을 의학석사 학위논문으로 제출함

2021년 2월

서울대학교 대학원
의과학과 면역학 전공

정 재 현

정재현의 의학석사 학위논문을 인준함
2021년 2월

위 원 장 정 두 현 (인)
부위원장 최 윤 수 (인)
위 원 이 원 우 (인)

Abstract

Idiopathic pulmonary fibrosis (IPF) is the most common interstitial lung disease that results from progressive fibrosis in the lung for an undefined reason. While IPF patients are susceptible for pulmonary bacterial infection that worsen fibrosis, IPF patients are symptomless or irrelevant for exacerbating for pulmonary viral infection. Given that type I interferon (IFN-I) production increases in renal epithelial cells during renal fibrosis, I hypothesized that IFN-I-dependent antiviral pathways might be induced by IPF conditions, which subsequently could provide resistance to following viral infections. This study revealed that mice were resistant to intranasal influenza virus infection IFN-I-dependently when treated with bleomycin (BLM) to develop pulmonary fibrosis. IFN-I mediated protection in BLM-treated lung appears to depend on activation of STING/TBK1/IRF3 pathway in lung and recruited plasmacytoid dendritic cells (pDC), as pDC depletion led to curtailed anti-viral responses of the BLM-treated mice. Using BLM-induced pulmonary fibrosis model, these data suggests asymptomatic of viral infection in IPF patients might be associated with activated STING/TBK1/IRF3 pathway and recruited pDCs that results increased IFN-I expression.

Keyword: Idiopathic pulmonary fibrosis, Type I interferon, Influenza virus, Plasmacytoid dendritic cell.

Student Number: 2018-26472

Table of Contents

List of figures

Introduction

Interstitial lung disease (ILD) is disease characterized by excessive cell proliferation, inflammation, and fibrosis in lung interstitium [1]. ILDs include chronic hypersensitivity, pulmonary sarcoidosis, and idiopathic pulmonary fibrosis (IPF) [1]. IPF is one of most common ILD with progressive and chronic fibrosis in lung and causative factors are mostly unknown [1]. IPF patients are usually more than 65 years old and survive 2~5 years after diagnosis [2]. Bacteria such as *Streptococcus aureus* or *Mycobacterium tuberculosis* are detected from bronchoalveolar lavage fluid (BALF) of IPF patients more frequently than healthy individuals and the presence of these bacteria are associated with aggravated disease outcome, but also role of bacteria in IPF pathogenesis is well defined [3, 4]. Whereas, the effect of pulmonary viral infection in IPF patients are still obscure. It was reported that viral infection affects IPF pathology, but other studies also reported asymptomatic viral infection in IPF patients [5-7]. In the current study, I asked why viral infections have less impact on IPF patients compare to bacterial infection. To answer this question, I sought to find the mechanism which provides resistance to viral infection after onset of IPF.

Bleomycin (BLM) has been used for anti-cancer drug and it has an

epidermal toxicity which induces fibrosis [8]. Researchers utilize BLM to induce pulmonary fibrosis animal model by using pulmonary toxicity of BLM [9]. Mouse exposed to BLM in lung releases TGF-β which is a major cytokine to stimulate fibroblast to repair damaged tissue that results in increased hydroxylproline and thickened alveoli in lung [10, 11].

Influenza virus is causative agent of the most common pulmonary infections and has a negative-RNA genome which is composed of 8 gene segments [12]. Pathology of influenza virus is characterized by increased secretion of pro-inflammatory cytokines, more frequent infiltration of immune cells, and alveolar dysfunction caused by loss of host cell integrity by infection [13]. I adopted influenza virus as a respiratory viral infection tool in my current study as this system is the most well defined mouse pulmonary viral infection model.

When infected with influenza virus, immunity defenses host from the invading virus by sensing pathogen associated molecular patterns (PAMP). Recognition of PAMP results in the expression of type I interferon (IFN-I) which takes crucial part of anti-viral immune responses [14]. Invaded virus is sensed by several receptors, such as toll like receptor (TLR), retinoic acid-inducible gene I (RIG-1), and mitochondrial antiviral signaling protein (MAVS) [15]. When IFN-I is produced by virus-infected cells, it binds to IFN-I receptor

(IFNAR) to initiate IFN-stimulated gene (ISG) expression which represses viral expansion in host cells and activates anti-viral immunity [15]. In addition to PAMP, damage associated molecular patterns (DAMP), such as nuclear acid, lipid, and metabolites released from injured or stressed cells are recognized by cells via TLR, RIG-I-receptor (RLR), NOD-like receptor (NLR) and cause inflammation [16]. Released DNA fragments from injured cells bind to cyclic GMP-AMP synthase (cGAS) and it activates stimulator of IFN gene (STING) which consequently produces IFN-I to IFN-I-dependent immune responses [16].

In the lung, diverse cells produce IFN-I including alveolar macrophages, alveolar epithelial cells, and dendritic cells [17]. In particular, plasmacytoid dendritic cells (pDCs) are known for abundant IFN-I producing cells as well as various cytokines such as IL-6, IL-12 and chemokines, which cover wide range of immune responses [18]. pDCs control early viral propagation by producing IFN-I and regulates apoptosis or necrosis-induced tolerance by secreting IL-10 [18, 19]. Detection of released DNA from injured skin activates pDCs and contribute recovery of lesion [20, 21]. However, pDC may become tolerogenic under uncontrolled activation and down-regulates IFN-I production to allow the progression of cancer or autoimmune diseases [18].

Chronical lupus nephritis is associated with renal fibrosis, which was associated with increased IFN-I production in tubular cells [22]. I hypothesized that pDC-mediated IFN-I production is responsible for viral resistance in IPF patients. I induced pulmonary fibrosis using BLM and observed increased IFN-I production in early point of virus infection. Up-regulation of IFN-I was associated with reduced pro-inflammatory cytokines and viral burden. Induction of IFN-I in BLM-treated mice was STING/TBK1/IRF3-dependent manner and was associated with increased pDCs. My results suggest that BLM treatment elevates IFN-I response and provides protection against viral infection.

Materials & Methods

Animal model

Specific pathogen-free (SPF) eight-week-old C57BL/6 female mice (18 ~ 20 g) were purchased from Charles River Laboratories (Orient Bio Inc., Sungnam, Korea) and IFNAR1 KO mice were bred and housed in Kangwon university animal laboratory center (LML-15-513). All protocols were approved by the Institutional Animal Care and Use Committee of Kangwon Nation University (Permit Number: KW-200131-2). To induce the pulmonary fibrosis, mice were anesthetized by injecting 100 μl of ketamine (25 mg/ml) and xylazine (2 mg/ml) mixture. Then 1 mg/kg of bleomycin (Merck) dissolved in 30 μl PBS was injected intranasally (i.n.). On day 14, mock- or BLM-treated mice were anesthetized and infected with 1 $\times$ 10^3 (sub-lethal) or 1 $\times$ 10^5 (lethal) PFU of A/Puerto Rico/8/34 (A/PR8) in 20 μl PBS by i.n.

Influenza virus propagation

SPF hen's eggs were purchased from Charles River laboratories (Orient Bio Inc. Sungnam, Korea) and incubated for 11 days. Five embryonated eggs were inoculated with 100 μl of virus stock into allantoic fluid. The allantoic fluid were harvested after 5 days of incubation at 37℃.

Bronchoalveolar lavage fluid (BALF)

After sacrificing mice, trachea was exposed and catheter was inserted to flush the lung with 1 ml of PBS. BALF samples were centrifuged at 14,000 rpm for 1 min to completely remove cells and supernatant was collected.

H&E staining

Lung was extracted and embed in paraffin. Lung was sectioned into 4 μm thick and stained with hematoxylin & eosin.

Total lung immune cell isolation

Lung was extracted and chopped using scissors. Tissue sample was incubated with 10 ml of digestion buffer containing RPMI-1640 (Gibco), 3% heat-inactivated fetal bovine serum (FBS) (Gibco), 10 mM HEPES (Gibco), 1% penicillin-streptomycin (Gibco), 400 U/ml of collagenase D (Roche) and 0.01 mg/ml DNase I (Roche) in shaking incubator at 37℃ under 200 rpm for 1 hr. Cells were collected in PBS containing 10 mM EDTA and spun at 500 g for 5 min. Cells were resuspended with 1 ml of RBC lysis buffer and incubated for 1 min at room temperature (RT). Cells were washed using PBS before use.

Hydroxyproline assay

Lung was weighted and homogenized with dH_2O. Hydroxyproline in sample homogenate was measured Hydroxyproline assay kit (Abcam) following manufacturer's instruction.

Enzyme linked immunosorbent assay (ELISA)

IL-6, CCL2, TNF-α, IFN-γ, IL-12p40 (Thermo fisher, uncoated plate) and CXCL1 (R&D system) were measured by ELISA kit following manufacturer's instruction.

mRNA quantification

Total mRNA was extracted from lung using TRIzol (Invitrogen) following manufacturer's instruction. mRNA was reverse-transcribed using reverse transcriptase (Promega). cDNA was amplified by using SYBR green pre-MIX (Promega). Target RNA expression level was normalized with *Gapdh* expression. Following primers used for quantitative reverse transcription polymerase chain reaction (Table 1). Primers were synthesized by Macrogen Inc. (Seoul, South Korea).

Table 1

Gene	Forward (5' → 3')	Reverse (5' → 3')
Gapdh	CCCCAGCAAGGACACTGAGCAA	GTGGGTGCAGCGAACTTTATTGATG
Ifna	TGATGAGCTACTACTGGTCAGC	GATCTCTTAGCACAAGGATGGC
M2	GACCAATCCTGTCACCTCTGA	AGGGCATTTTGGACAAAGCGTCTAAA

Plaque assay

Whole lung was extracted and weighted. Lung was homogenated using plastic bead containing 2 ml tube with PBS. Homogenated tissue was centrifuged at 12,000 rpm for 5 min and supernatant was collected. Collected supernatant was stored at −80℃ before use. A549 cells were cultured in DMEM (Corning) supplemented with 1× antibiotic−antimycotic (A/A) (Gibco) and 10% heat−inactivated FBS. A549 cells were seeded 1 × 10^6 per well in 6−well plate (Corning) a day before analysis. Samples were serially diluted in 1 ml of DMEM supplemented with 1% A/A before incubated with PBS washed cells at 37℃, 5% CO_2 for 1 hr. Inoculated cells were washed with PBS and overlaid with DMEM supplemented with 1% A/A and 1% agarose. After incubation for 5 days at 37℃, 5% CO2, overlay was removed and fixed with 4% formalin for overnight at RT. Fixed cells were stained with 1% crystal violet for 30 min at RT and washed with 1% acetic acid 20 min for 3 times before count plaques.

Western blot

Lung tissue was lysed with protein extraction solution (iNtRON) containing 1× proteases inhibitor cocktail (Sigma) and 1× phosphatase inhibitor cocktail (GenDEPOT). The lysate was centrifuged at 4,000 rpm for 10 min, then supernatant was collected. Protein concentration in the supernatant was measured using BCA protein assay kit (Thermo Fisher). Samples (10 μg) were loaded on 10% polyacrylamide gel and run at 120V for 90 min with Mini-PROTEAN Tetra Cell (Bio-Rad). To transfer proteins in the gel to nitrocellulose membrane, Trans-Blot SD (Biorad) was used and run at 250 mA for 90 min. Membrane was blocked with 5% skim milk (w/v) in 1× TBS-T (20 mM Tris Base, 150 mM sodium chloride, and 0.05% Tween-20, pH 7.6) for mouse anti-mouse antibody, 5% BSA and 0.05% Tween-20 in 1× TBS for rabbit anti-mouse antibody. Primary antibodies used in this study are rabbit anti-STING (#13647, Cell signaling), rabbit anti-phospho-STING (#85735, Cell signaling), rabbit anti-TBK1/NAK (#3013, Cell signaling), rabbit anti-phospho-TBK1/NAK (#5483, Cell signaling), rabbit anti-IRF3 (#4302, Cell signaling), rabbit anti-phospho-IRF3 (#4947, Cell signaling) and mouse anti-β-actin (sc-47778, Santa Cruz). Primary antibodies were used following manufacturer's instruction. Membranes washed 3 times with 0.05% Tween-20 in 1

× TBS each for 20 min at RT. Then membranes were incubated with goat-anti-rabbit-HRP-conjugated antibody which was diluted in 2.5% BSA containing 0.05% Tween-20 in 1× TBS (1: 2500) or mouse-anti-mouse-HRP-conjugated antibody which was diluted in 5% skim milk in 1× TBS-T for 2 hr at RT. The membranes were washed 3 times with 0.05% Tween-20 in 1× TBS (1: 5000) for 20 min at RT. Blots were detected using chemi-luminescent reagents (G-BIOSCIECNE) and were captured with PXi gel doc system (Biorad). Arbitrary unit was determined using ImageJ (NIH).

Flow cytometry

Collected lung immune cells were incubated with anti-CD16/CD32 (2.4G2). Cell surface markers were stained for 30 min at 4℃ protected from light using different combination of fluorescent-conjugated antibodies: CD11c (HL3), PDCA1 (HM1.2), CD45 (30-F11), CD4 (RM4-5), CD8 (53-6.7), NK1.1 (PK136) and CD49b (DX5) are purchased from Biolegend. B220 (RA3-6B2) and lineage (145-2C11, M1/70, RA3-6B2, TER-119, RB6-8C5) are purchased from BD. Stained cells are read using FACS Verse (BD Bioscience). The data was analyzed with FlowJo (BD Bioscience) version 10.5.3.

In vivo cell depletion

300 μg of αNK1.1 (PK136) and 300 μg of αCD8 (Lyt2.1) were injected intraperitoneally (i.p.) 7, 4, 1 day before A/PR8 infection. 80 μg of αCD317 (PDCA-1) was injected i.p. 1 day before, 6, 13 days after BLM treatment and 3 days post A/PR8 infection. All depletion antibodies are purchased from BioXcell.

Results

BLM-treated mice resist to influenza virus infection.

I adopted well established BLM and A/PR8 mouse model to study the mechanism between IPF and pulmonary viral infection. First, I confirmed induction of pulmonary fibrosis by BLM treatment. Increased hydroxylproline, a major protein collagen found in fibrotic lung, and thicken alveolar wall is hallmark of lung fibrosis [11]. I measured hydroxyproline level by Hydroxyproline assay kit and determined alveolar wall thickening by H&E stained slide from lung sample on 14 days after BLM treatment. Increased hydroxyproline and thickened alveolar wall was detected in BLM-treated mice than control mice (Fig. 1A, B).

Once I confirmed fibrosis in BLM-treated mice, I infected sub-lethal dose of A/PR8 (1×10^3 plaque forming unit [PFU]) by i.n. after anesthesia and monitored body weight for 8 days. BLM-treated mice lost body weight up to 5% while PBS-treated mice lost nearly 20% (Fig. 2A). To check the mortality of mice, I infected BLM-treated mice with lethal dose of A/PR8 (1×10^3 PFU) and monitored for 14 days. PBS-treated mice showed lower survival rate (10%) compare to BLM-treated mice (85%) (Fig. 2B). It was reported that A/PR8 infection induces exacerbation of pro-inflammatory cytokine and aggravates pulmonary inflammation [23]. I hypothesized that

attenuated viral infection in BLM-treated mice are related with attenuated pro-inflammatory cytokine production. BALF was collected 3 days after infection and cytokines levels were determined. TNF-α, CCL2, IFN-γ, and CXCL1 were significantly decreased in BLM-treated mice than control mice (Fig. 3A~D), whereas, the secretion of IL-6 and IL-12p40 were comparable in both groups (Fig. 3E, F). From these data, I confirmed the anti-viral effects was induced by BLM treatment in mice and showed its possible connection with attenuated inflammatory cytokine production.

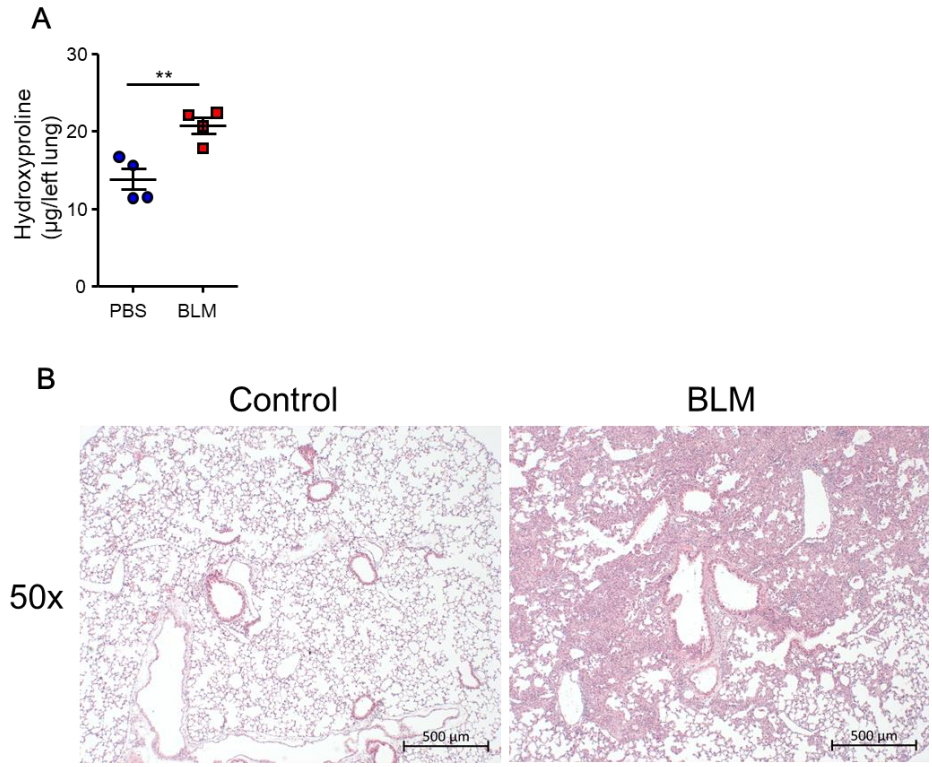

Figure 1. Bleomycin (BLM) induces pulmonary fibrosis.

Mice were treated with 1 mg/kg of BLM in 30 μl of PBS i.n. (A) Hydroxyproline in lung homogenate and (B) H&E stained lung section was imaged at 14 days after BLM treatment.

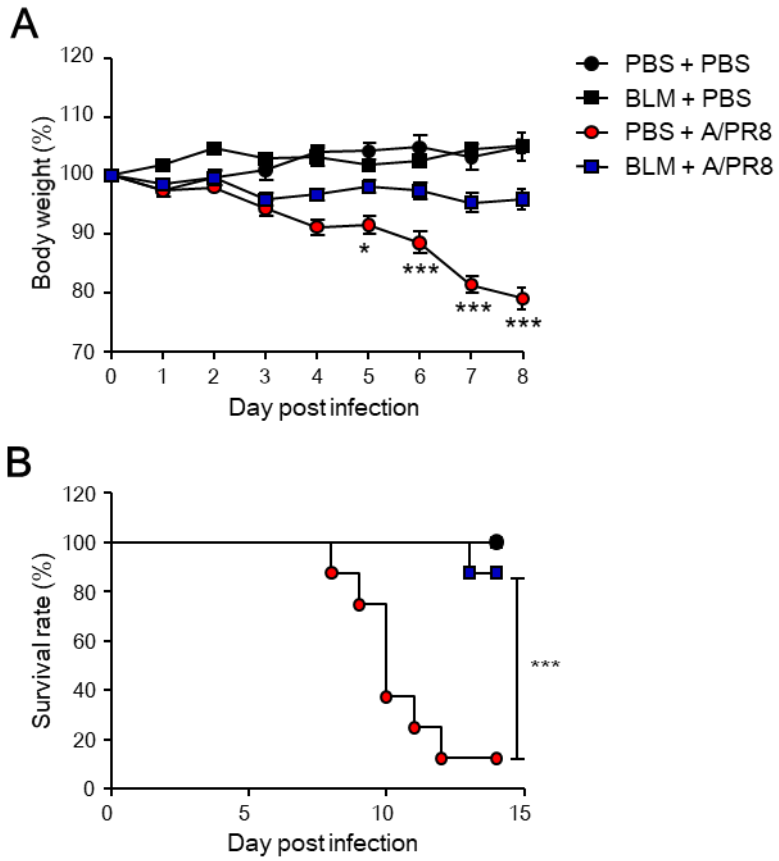

Figure 2. Bleomycin (BLM)-treated mice have resistance to A/PR/8/34 (A/PR8) infection.

(A) BLM-treated mice were infected with sub-lethal dose (1×10^3 PFU) of A/PR8 by i.n. and monitored body weight for 8 days. (B) BLM-treated mice were infected with lethal dose (1×10^5 PFU) of A/PR8 by i.n. and survival of mice were monitored for 14 days.

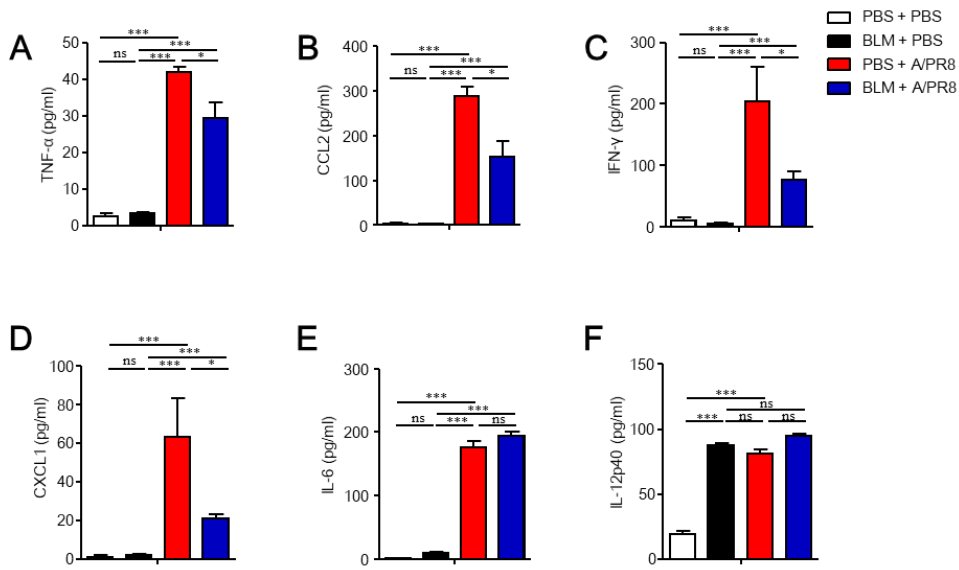

Figure 3. Inflammatory cytokines are decreased in A/PR/8/34 (A/PR8) infected BLM-treated mice.

Mice were infected with sub-lethal dose (1×10^3 PFU) of A/PR8 by i.n. and bronchoalveolar lavage fluid (BALF) was extracted at 3 days after infection. (A) TNF-α, (B) CCL2, (C) IFN-γ, (D) CXCL1, (E) IL-6 and (F) IL-12p40 in BALF were measured by ELISA.

NK cells and $CD8^+$T cells are not related with A/PR8 resistance in BLM-treated mice.

IL-12p40, a subunit of IL-12 family cytokine, were increased in both of A/PR8 infected BLM-treated and its control mice as well as BLM control group (Fig. 3F). IL-12p40 is a subunit of IL-12p70 that activates cytotoxic lymphoid cells like natural killer (NK) cells and $CD8^+$T cells [23-25]. So I analyzed NK cells and $CD8^+$T cells in lung after 1×10^3 PFU of A/PR8 infection to BLM-treated mice. Percentage of NK cells and $CD8^+$ T cells in A/PR8 infected groups are decreased than un-infected (Fig. 4A). Total lung cells are increased after BLM treatment in both control and infected groups (Fig. 4B). $CD8^+$T cells were significantly increased after A/PR8 infection in BLM-treated mice, however, NK cells number was not affected (Fig. 4C, D). To check cytotoxic lymphoid cells contribute to anti-viral phenotype, I depleted NK cells and $CD8^+$T cells by treating depletion antibody on 7, 4, 1 days before 1×10^3 PFU of A/PR8 infection. Then body weight was monitored for 7 days and sacrificed to measure titer of A/PR8 in lung. As a result, depletion of cytotoxic lymphoid cells did not affected morbidity of BLM-treated A/PR8-infected mice (Fig 5A, B). Expectedly, lung viral titer at 7 d.p.i was reduced in BLM-treated mice compare to control mice in the absence of cytotoxic lymphoid cells (Fig. 5C). This data indicates

that increased NK cells and $CD8^+$T cells are dispensable for anti-viral effects in BLM-induced pulmonary fibrosis mice.

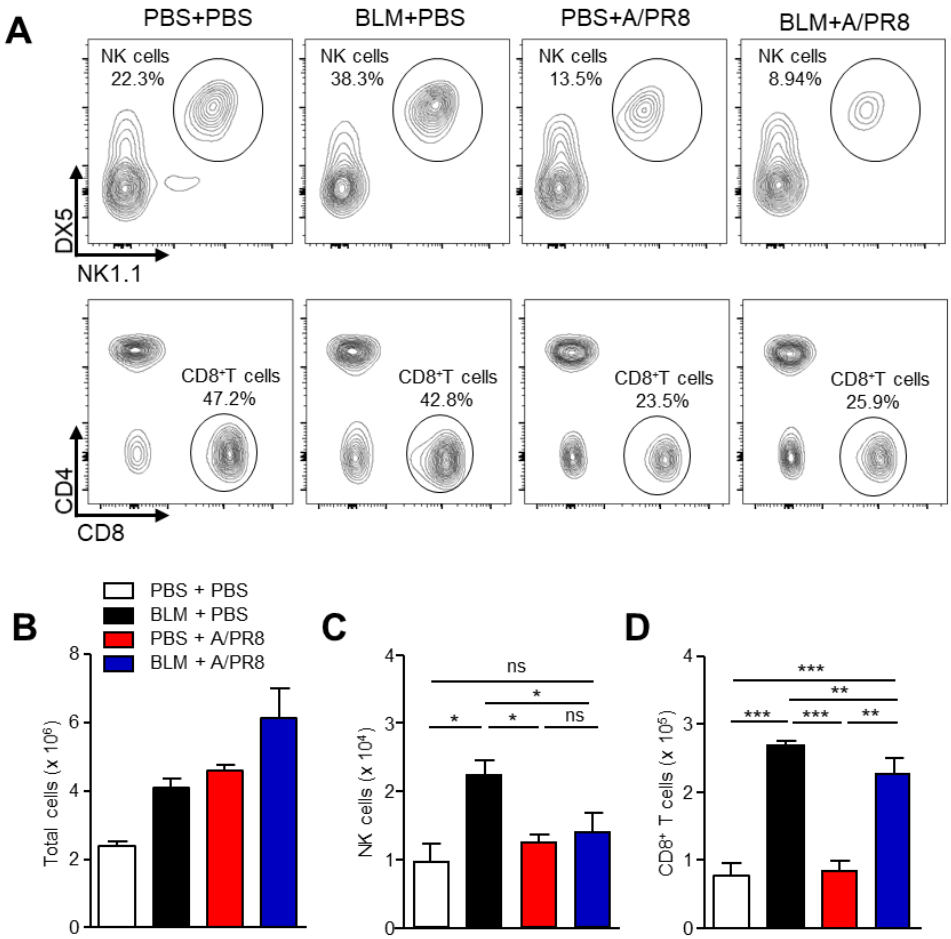

Figure 4. Natural killer (NK) cells and $CD8^+$T cells are increased in A/PR/8/34 (A/PR8) infected BLM-treated mice.

Mice were infected with sub-lethal dose (1×10^3 PFU) of A/PR8 by i.n. and lung cells were analyzed at 3 days after infection. (A) FACS plots of NK cells were gated from $CD45^+Lin^-$ and $CD8^+$T cells were gated from $CD45^+CD3^+$. (A) Total cells, (C) NK cells, (D) $CD8^+$T cells number are shown.

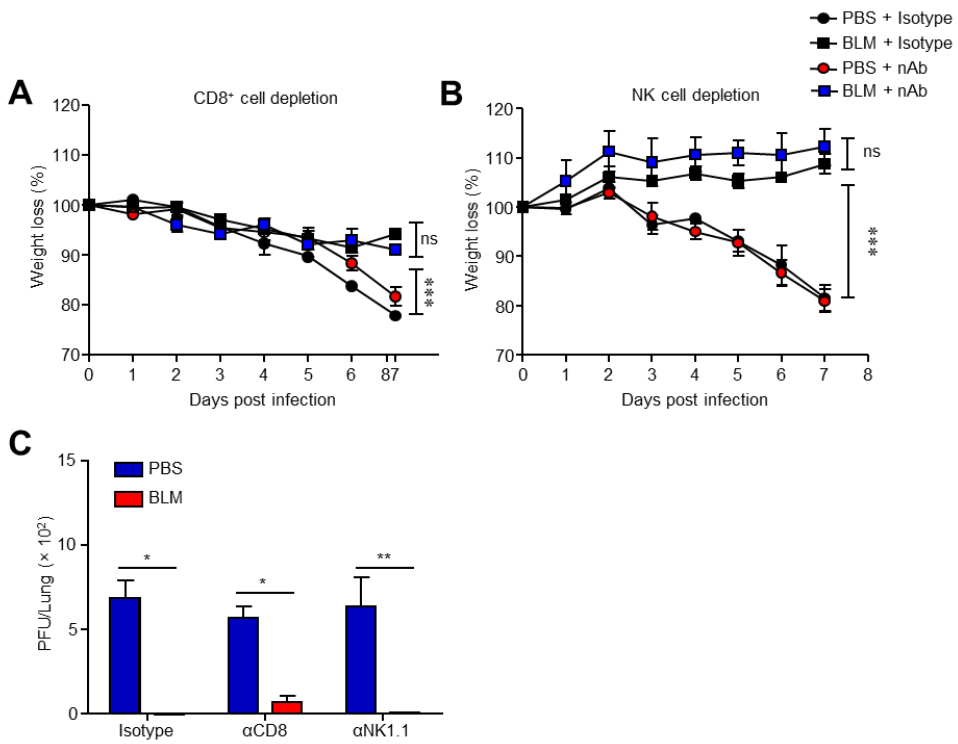

Figure 5. Deposited natural killer (NK) cells and $CD8^+$T cells in bleomycin (BLM)-treated mice are dispensable for A/PR/8/34 resistance.

Depletion antibodies of NK cells and $CD8^+$T cells are treated by i.p 7, 4, 1 days before sub-lethal dose (1×10^3 PFU) of A/PR8. (A) $CD8^+$T cells-depleted mice and (B) NK cells-depleted mice body weight was monitored for 7 days. (C) Virus titers in lung was measured by plaque forming assay at 7 days after infection.

BLM treatment increases IFN-I-dependent viral resistance.

IFN-I is crucial cytokine to repress viral replication in host cells via ISG expression [26]. I hypothesized that anti-viral effects in BLM-treated mice are related with upregulated IFN-I expression. To test this, I infected BLM-treated mice with 1×10^5 PFU of A/PR8 and analyzed IFN-I gene expression level at 1 day after infection. *Ifna* transcription level was higher in BLM-treated mice than PBS-treated (Fig. 6A). To confirm that virus propagation is hindered by IFN-I, I measured *M2*, viral gene that coding matrix protein, 2 days after 1×10^5 PFU of A/PR8 infection. *M2* gene level was lower in BLM-treated mice than PBS-treated, indicating negative correlation between IFN-I induction and virus propagation in the lung (Fig. 6B). Next, I used IFNAR1 knockout (KO) mice to confirm that BLM treatment fail to induce anti-viral response in IFN-I signaling-deficient environment. Both IFNAR1 KO and WT mice were treated with BLM and followed by infection with sub-lethal (1×10^3 PFU) dose of A/PR8 to monitor body weight for 7 days. BLM treatment to IFNAR1 KO mice did not show any reduction in weight loss compared to PBS-treated IFNAR1 KO mice (Fig. 7A). When viral titer was assessed 2 days after 1×10^5 PFU of A/PR8 infection, BLM-treated WT mice showed reduced viral burden compare to PBS control while BLM treatment to IFNAR1 KO showed

comparable viral burden with control IFNAR1 KO mice (Fig. 7B). These data indicate that BLM-treated mice acquire anti-viral resistance in IFN-I-dependent manner.

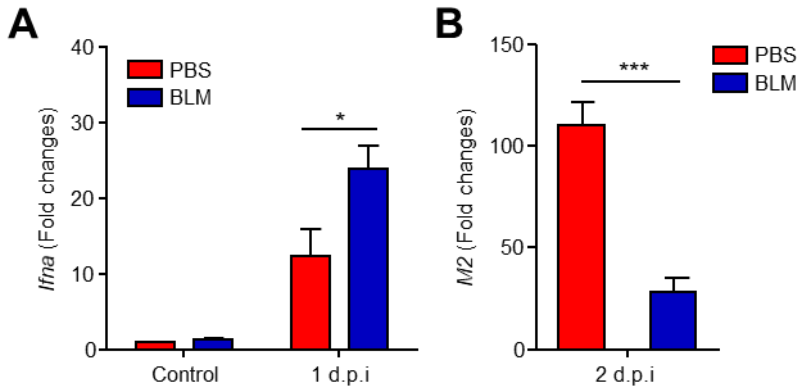

Figure 6. Bleomycin (BLM)-treated mice rapidly expressed type I interferon (IFN-I) against A/PR/8/34 (A/PR8) infection.

BLM-treated mice were infected with lethal dose (1×10^5 PFU) of A/PR8 by i.n. (A) *Ifna* gene expression level in lung was analyzed 1 day after infection. (B) *M2*, one of A/PR8 genes, expression level in lung was analyzed 2 day after infection.

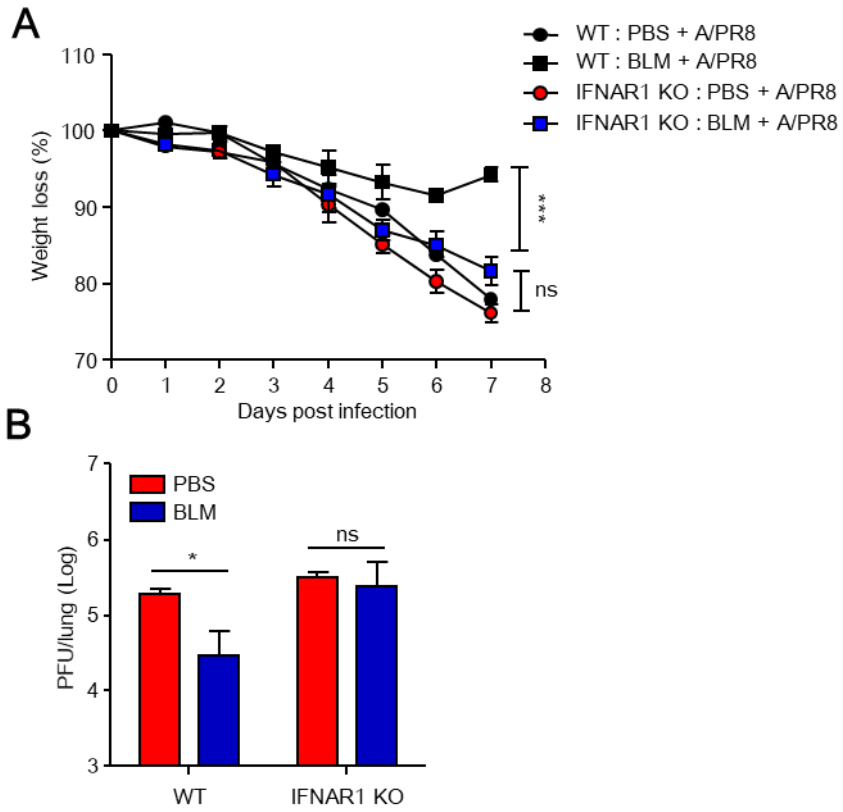

Figure 7. A/PR/8/34 (A/PR8) is controlled via type I interferon (IFN-I)-dependent manner in BLM-treated mice.

Bleomycin (BLM)-treated Wild type (WT) and IFN-I receptor 1 (IFNAR1) knock out mice were infected with A/PR8. (A) Mice were infected with lethal dose (1×10^5 PFU) of A/PR8 by i.n and virus titer in lung was measured by plaque assay at 2 day after infection. (B) Mice were infected with sub-lethal dose (1×10^3 PFU) of A/PR8 by i.n. and monitored body weight for 7 days.

BLM treatment activates cGAS-STING pathway and increases pDCs that contribute A/PR8 resistance.

BLM injures alveolar epithelial cells and causes necrosis-derived DNA fragments [27, 28]. Released self-DNA binds to cGAS and activates STING, consequently phosphorylates IRF3 that initiates IFN-I expression [29]. When cGAS-STING pathway-related proteins in the lung was examined 7 days after BLM treatment, prominent levels of STING, phosphorylated (p)-STING, p-TBK1 and p-IRF3 were observed in lung of BLM-treated mice. These up-regulated expression and phosphorylation indicates activation of cGAS-STING pathway by BLM treatment (Fig. 8A, B). Alveolar epithelial cells, macrophage and pDCs are known to produce IFN-I upon viral infection. Among these, pDCs are dominant IFN-I producing cells that can be stimulated by viral infection or release self-DNA through cGAS-STING pathway [30-33].

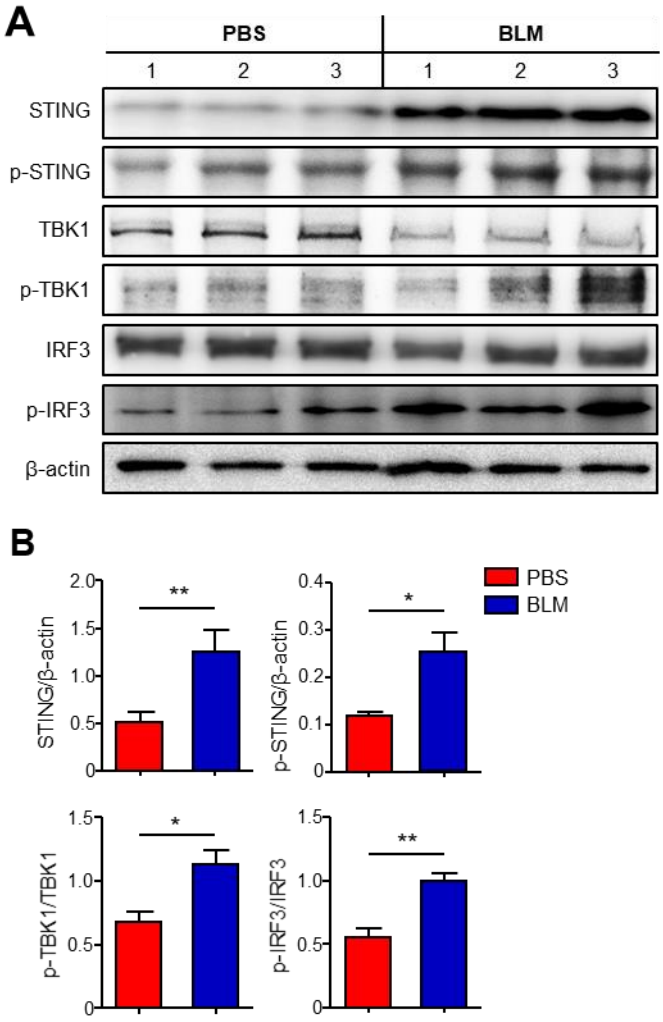

Figure 8. cGAS-STING pathway in lung is activated after bleomycin (BLM) treatment.

Mice were treated with BLM by i.n. and lung was analyzed after 7 days. (A) Immunoblot of STING, phosphorylated (p)-STING, TBK1, p-TBK1, IRF3, p-IRF3 and β-actin in lung homogenates. (B) STING and p-STING was normalized with β-actin and p-TBK1, p-IRF3 was normalized with each of total form relatively.

After 7 days BLM treatment, percentage of pDCs in BLM-treated mice lung was comparable with one that in PBS-treated mice (Fig. 9A, B), however, absolute pDC number were higher in BLM-treated, suggesting pDCs might responsible for enhanced IFN-I expression after BLM treatment (Fig. 9B, C). To prove this hypothesis, I depleted pDCs by treating depletion antibody (αPDCA1) on 15, 7, 1 days before 1×10^3 PFU A/PR8 infection and monitored body weight for 8 days. pDC depletion in BLM-treated mice significantly decreased body weight compared to BLM-treated isotype control (Fig. 9D). These data suggest that BLM-induced pulmonary damage activates cGAS-STING pathway that produces IFN-I secretion and it is related to increased pDCs numbers which contribute to A/PR8 resistance (Fig. 10).

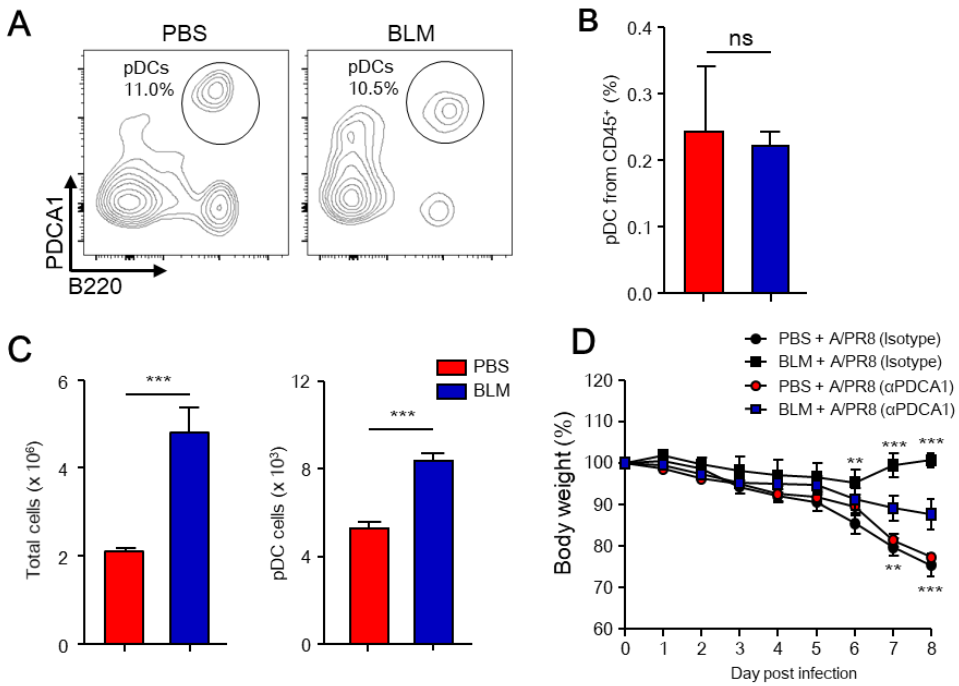

Figure 9. Plasmacytoid dendritic cells (pDCs) are increased after bleomycin (BLM)-treatment and it contributes to A/PR/8/34 (A/PR8) infection.

(A) FACS plot of pDCs were gated from $CD45^{+}CD11c^{+}$ and (B) pDCs percentage from $CD45^{+}$ are shown. (C) Total and pDCs cells number in lung was analyzed 7 days after BLM treatment by i.n. (D) Depletion antibody of pDC was treated 15, 8, 1 day before and 3 days after sub-lethal dose (1×10^{3} PFU) of A/PR8 infection by i.p. and monitored body weight for 8 days.

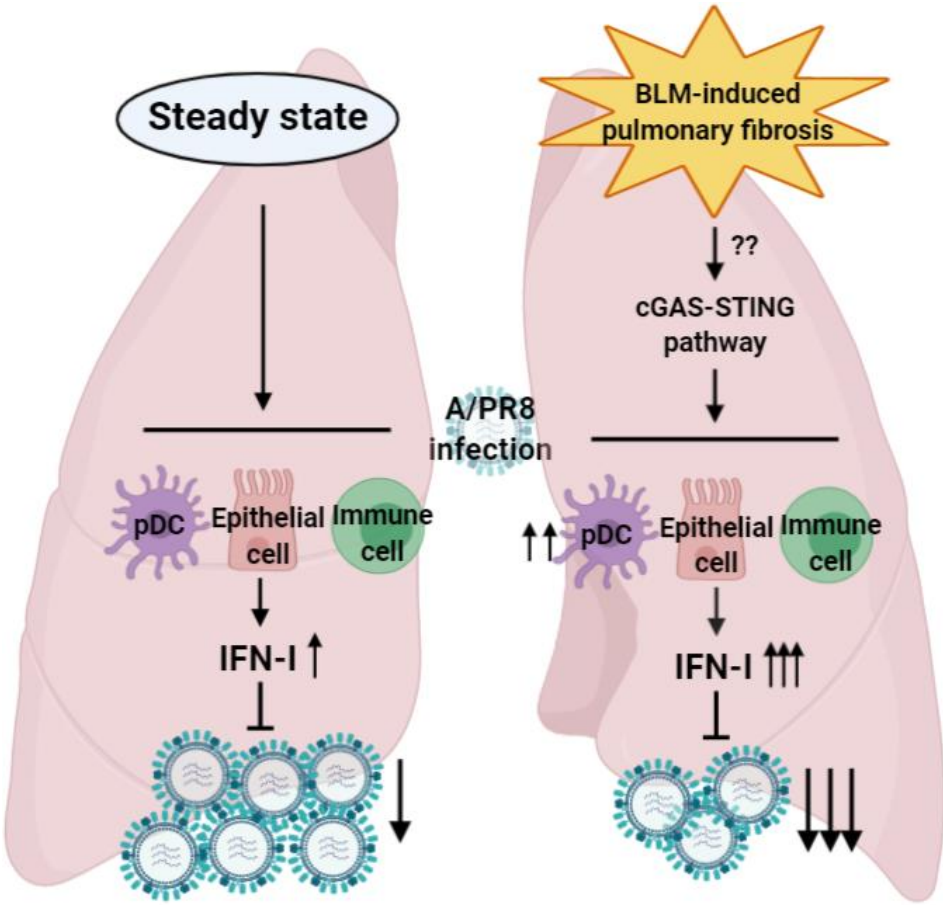

Figure 10. Bleomycin treatment activates cGAS−STING pathway and recruits pDCs which provide type I interferon−dependent resistance to A/PR/8/34 infection. Image is created in BioRender.com

Discussion

Some viruses including cytomegalovirus, Epstein-Barr virus and human herpesvirus are known for increasing development of IPF [6]. The pathology of influenza virus infection in IPF patients is controversial and the mechanism how influenza virus avoid IPF exacerbation is remained unclear [5-7, 34]. My data suggest that induced IFN-I immune response in IPF patients enhances anti-viral responses and contribute asymptomatic or attenuated pathology of viral infection.

Diverse innate immune pathways such as TLR, RIG-I-like receptor (RLR) sense A/PR8 to inhibit its replication via expressing IFN-I [35]. cGAS-STING pathway is mainly activated self-DNA or dsDNA viruses, but it is studied that cGAS-STING pathway also takes role in protecting host from RNA virus infection [36, 37]. IFN-I expression level in BLM-treated mice lung was higher after A/PR8 infection, however, whether increased IFN-I gene expression is controlled by cGAS-STING dependently is unknown. Also, how the activated STING/TBK1/IRF3 contributes to anti-viral effects in BLM-treated mice and which factors could result the anti-viral effects from the signal are associated need to be studied in further study. STING produces IFN-I by phosphorylating IRF3 in canonical

pathway, however in non-canonically, IFN-I production is proceeded via phosphorylating NF-κB rather than IRF-3 [38]. Further studies are required to confirm that STING/TBK1/IRF3 signaling after BLM treatment is responsible for viral resistance and whether RIG-I, TLR signals and NF-κB are also involved in IFN-I expression. In addition, STING/TBK1/IRF3 signaling molecules were investigated with whole lung tissue, thus further studies are required to determine which cells dominantly activate this signaling pathway. In different tissue fibrosis model using cisplatin for inducing renal fibrosis suggests that cisplatin-exposed tubular cell lines increase STING pathway phosphorylates TBK1 and p65 rather than IRF3 which results in NF-κB expression but not IFN-I [39]. STING pathway related with fibrosis seems to be activated differently dependent on organs. Increased IFN-I responses are observed in tubular cells of lupus nephritis (LN) patients [40] that suggests enhanced IFN-I activity may be associated with renal fibrosis in LN. However, the mechanism of enhanced IFN-I activity after pulmonary fibrosis was not fully identified. Mechanism of up-regulated IFN-I activity in LN-induced renal fibrosis and BLM-induced pulmonary fibrosis might be differently developed in that different tissue and disease. Thus, further study is required to elucidate co-relation between increased IFN-I in pulmonary fibrosis.

pDCs produce robust IFN-I against microbe infection to initiate immune responses [31]. pDCs-derived IFN-I modulates lipid metabolic and biosynthesis that increases 2, 5-hydroxycholesterol repressing viral replication [43-45]. Non-hematopoietic cells up-regulate fatty acid oxidations that inhibit A/PR8 infection via receiving pDC-derived IFN-I [46]. Hence, it seems that pDCs controls viral infection in various way using IFN-I-related immune regulation. Influenza virus inhibits IFN-I-stimulated and lipid-mediated viral resistance by expressing non-structural (NS) 1 protein [47]. While I observed increased IFN-α mRNA expression in whole lung of BLM-treated mice groups, future studies are required to determine the origin of IFN-a production in the lung given that diverse innate cells, such as alveolar macrophage, alveolar epithelial cells and dendritic cells are able to respond to A/PR8 infection [17]. In this study, pDCs-derived IFN-I take a role in controlling A/PR8 replication in BLM-induced pulmonary fibrosis model.

In general, cytotoxic lymphocytes are important at defending viral infection [48]. I observed that NK cells and $CD8^+$T cells were recruited in the lung after BLM treatment. Depletion of either NK cells or $CD8^+$T cells failed to control A/PR8 infection. In previous study, NK cells and $CD8^+$T cells are recruited to the lung to attenuate

BLM-induced pulmonary inflammation [49, 50]. Recruited NK cells and $CD8^+$T cells restore BLM-induced inflammation by stimulating fibroblasts to produce more matrix [51]. This suggests recruited cytotoxic lymphocytes are recruited for repairing tissue damage rather than contributing anti-viral effects which is dominantly regulated by IFN-I-dependent manner.

Except figure 2A and B, controls for un-infected groups were not included in other experiments. Experiments that couldn't adjust un-infected control groups will be reinforced via reproducing experiments. Increased pro-inflammatory cytokines and chemokines recruit inflammatory cells that cause tissue damage [23]. To solidify data for decreased pathology in BLM-treated group, experiments for correlation between inflammatory cytokines with immune cells and pulmonary histopathology need to be performed.

pDC depletion antibody was used in this experiments, the protection against A/PR8 infection was partially reduced in comparison which is almost complete loss of protection in IFN-I deficient mice. It could result from incomplete depletion of pDCs, or could be due to compensatory IFN-I production by other types of cells. Though I treated depletion antibody of either NK cells or $CD8^+$T cells before A/PR8 infection, it needs to check population of those cells before A/PR8 infection to confirm which cells contribute

to the resistance against A/PR8 infection. Adding data for evidence of depleted target cells needs to solidify with reproduces.

Overall, BLM treatment activated STING/TBK1/IRF3 pathway and recruited pDCs which results rapid IFN-I production against A/PR8 infection in BLM-induced pulmonary fibrosis model. This study may explain why IPF patients are relatively less susceptible to viral infection compare to bacterial infection and activated cGAS-STING pathway and pDCs might be responsible for this phenomenon.

Bibliography

[1] D. J. Lederer and F. J. Martinez, "Idiopathic Pulmonary Fibrosis," N Engl J Med, vol. 378, no. 19, pp. 1811-1823, May 10 2018, doi: 10.1056/NEJMra1705751.

[2] G. Raghu et al., "Idiopathic pulmonary fibrosis in US Medicare beneficiaries aged 65 years and older: incidence, prevalence, and survival, 2001-11," Lancet Respir Med, vol. 2, no. 7, pp. 566-72, Jul 2014, doi: 10.1016/S2213-2600(14)70101-8.

[3] M. J. Chung, J. M. Goo, and J. G. Im, "Pulmonary tuberculosis in patients with idiopathic pulmonary fibrosis," Eur J Radiol, vol. 52, no. 2, pp. 175-9, Nov 2004, doi: 10.1016/j.ejrad.2003.11.017.

[4] P. L. Molyneaux et al., "The role of bacteria in the pathogenesis and progression of idiopathic pulmonary fibrosis," Am J Respir Crit Care Med, vol. 190, no. 8, pp. 906-13, Oct 15 2014, doi: 10.1164/rccm.201403-0541OC.

[5] B. B. Moore and T. A. Moore, "Viruses in Idiopathic Pulmonary Fibrosis. Etiology and Exacerbation," Ann Am Thorac Soc, vol. 12 Suppl 2, pp. S186-92, Nov 2015, doi: 10.1513/AnnalsATS.201502-088AW.

[6] G. Sheng et al., "Viral Infection Increases the Risk of Idiopathic Pulmonary Fibrosis: A Meta-analysis," Chest, Nov 12

2019, doi: 10.1016/j.chest.2019.10.032.

[7] S. C. Wootton et al., "Viral infection in acute exacerbation of idiopathic pulmonary fibrosis," Am J Respir Crit Care Med, vol. 183, no. 12, pp. 1698-702, Jun 15 2011, doi: 10.1164/rccm.201010-1752OC.

[8] J. Hay, S. Shahzeidi, and G. Laurent, "Mechanisms of bleomycin-induced lung damage," Arch Toxicol, vol. 65, no. 2, pp. 81-94, 1991, doi: 10.1007/bf02034932.

[9] T. Liu, F. G. De Los Santos, and S. H. Phan, "The Bleomycin Model of Pulmonary Fibrosis," Methods Mol Biol, vol. 1627, pp. 27-42, 2017, doi: 10.1007/978-1-4939-7113-8_2.

[10] I. E. Fernandez and O. Eickelberg, "The impact of TGF-beta on lung fibrosis: from targeting to biomarkers," Proc Am Thorac Soc, vol. 9, no. 3, pp. 111-6, Jul 2012, doi: 10.1513/pats.201203-023AW.

[11] G. Izbicki, M. J. Segel, T. G. Christensen, M. W. Conner, and R. Breuer, "Time course of bleomycin-induced lung fibrosis," Int J Exp Pathol, vol. 83, no. 3, pp. 111-9, Jun 2002, doi: 10.1046/j.1365-2613.2002.00220.x.

[12] J. K. Taubenberger and J. C. Kash, "Influenza virus evolution, host adaptation, and pandemic formation," Cell Host Microbe, vol. 7, no. 6, pp. 440-51, Jun 25 2010, doi: 10.1016/j.chom.2010.05.009.

[13] R. R. Thangavel and N. M. Bouvier, "Animal models for

influenza virus pathogenesis, transmission, and immunology," J Immunol Methods, vol. 410, pp. 60-79, Aug 2014, doi: 10.1016/j.jim.2014.03.023.

[14] D. B. Stetson and R. Medzhitov, "Type I interferons in host defense," Immunity, vol. 25, no. 3, pp. 373-81, Sep 2006, doi: 10.1016/j.immuni.2006.08.007.

[15] F. McNab, K. Mayer-Barber, A. Sher, A. Wack, and A. O'Garra, "Type I interferons in infectious disease," Nat Rev Immunol, vol. 15, no. 2, pp. 87-103, Feb 2015, doi: 10.1038/nri3787.

[16] T. Gong, L. Liu, W. Jiang, and R. Zhou, "DAMP-sensing receptors in sterile inflammation and inflammatory diseases," Nat Rev Immunol, vol. 20, no. 2, pp. 95-112, Feb 2020, doi: 10.1038/s41577-019-0215-7.

[17] M. Swiecki and M. Colonna, "Type I interferons: diversity of sources, production pathways and effects on immune responses," Curr Opin Virol, vol. 1, no. 6, pp. 463-75, Dec 2011, doi: 10.1016/j.coviro.2011.10.026.

[18] M. Swiecki and M. Colonna, "The multifaceted biology of plasmacytoid dendritic cells," Nat Rev Immunol, vol. 15, no. 8, pp. 471-85, Aug 2015, doi: 10.1038/nri3865.

[19] J. Simpson, K. Miles, M. Trub, R. MacMahon, and M. Gray, "Plasmacytoid Dendritic Cells Respond Directly to Apoptotic Cells by

Secreting Immune Regulatory IL-10 or IFN-alpha," Front Immunol, vol. 7, p. 590, 2016, doi: 10.3389/fimmu.2016.00590.

[20] J. Gregorio et al., "Plasmacytoid dendritic cells sense skin injury and promote wound healing through type I interferons," J Exp Med, vol. 207, no. 13, pp. 2921-30, Dec 20 2010, doi: 10.1084/jem.20101102.

[21] R. Lande et al., "Plasmacytoid dendritic cells sense self-DNA coupled with antimicrobial peptide," Nature, vol. 449, no. 7162, pp. 564-9, Oct 4 2007, doi: 10.1038/nature06116.

[22] E. Der et al., "Tubular cell and keratinocyte single-cell transcriptomics applied to lupus nephritis reveal type I IFN and fibrosis relevant pathways," Nat Immunol, vol. 20, no. 7, pp. 915-927, Jul 2019, doi: 10.1038/s41590-019-0386-1.

[23] Q. Liu, Y. H. Zhou, and Z. Q. Yang, "The cytokine storm of severe influenza and development of immunomodulatory therapy," Cell Mol Immunol, vol. 13, no. 1, pp. 3-10, Jan 2016, doi: 10.1038/cmi.2015.74.

[24] T. Scharton-Kersten, L. C. Afonso, M. Wysocka, G. Trinchieri, and P. Scott, "IL-12 is required for natural killer cell activation and subsequent T helper 1 cell development in experimental leishmaniasis," J Immunol, vol. 154, no. 10, pp. 5320-30, May 15 1995. [Online]. Available:

https://www.ncbi.nlm.nih.gov/pubmed/7730635.

[25] C. J. Henry, D. A. Ornelles, L. M. Mitchell, K. L. Brzoza-Lewis, and E. M. Hiltbold, "IL-12 produced by dendritic cells augments CD8+ T cell activation through the production of the chemokines CCL1 and CCL17," J Immunol, vol. 181, no. 12, pp. 8576-84, Dec 15 2008, doi: 10.4049/jimmunol.181.12.8576.

[26] M. J. Killip, E. Fodor, and R. E. Randall, "Influenza virus activation of the interferon system," Virus Res, vol. 209, pp. 11-22, Nov 2 2015, doi: 10.1016/j.virusres.2015.02.003.

[27] D. R. Schwartz, G. E. Homanics, D. G. Hoyt, E. Klein, J. Abernethy, and J. S. Lazo, "The neutral cysteine protease bleomycin hydrolase is essential for epidermal integrity and bleomycin resistance," Proc Natl Acad Sci U S A, vol. 96, no. 8, pp. 4680-5, Apr 13 1999, doi: 10.1073/pnas.96.8.4680.

[28] H. Suzuki, K. Nagai, H. Yamaki, N. Tanaka, and H. Umezawa, "On the mechanism of action of bleomycin: scission of DNA strands in vitro and in vivo," J Antibiot (Tokyo), vol. 22, no. 9, pp. 446-8, Sep 1969, doi: 10.7164/antibiotics.22.446.

[29] Q. Chen, L. Sun, and Z. J. Chen, "Regulation and function of the cGAS-STING pathway of cytosolic DNA sensing," Nat Immunol, vol. 17, no. 10, pp. 1142-9, Sep 20 2016, doi: 10.1038/ni.3558.

[30] S. Makris, M. Paulsen, and C. Johansson, "Type I Interferons

as Regulators of Lung Inflammation," Front Immunol, vol. 8, p. 259, 2017, doi: 10.3389/fimmu.2017.00259.

[31] D. A. Chistiakov, A. N. Orekhov, I. A. Sobenin, and Y. V. Bobryshev, "Plasmacytoid dendritic cells: development, functions, and role in atherosclerotic inflammation," Front Physiol, vol. 5, p. 279, 2014, doi: 10.3389/fphys.2014.00279.

[32] C. Bode et al., "Human plasmacytoid dentritic cells elicit a Type I Interferon response by sensing DNA via the cGAS-STING signaling pathway," Eur J Immunol, vol. 46, no. 7, pp. 1615-21, Jul 2016, doi: 10.1002/eji.201546113.

[33] P. Fitzgerald-Bocarsly and D. Feng, "The role of type I interferon production by dendritic cells in host defense," Biochimie, vol. 89, no. 6-7, pp. 843-55, Jun-Jul 2007, doi: 10.1016/j.biochi.2007.04.018.

[34] T. Saraya et al., "Clinical significance of respiratory virus detection in patients with acute exacerbation of interstitial lung diseases," Respir Med, vol. 136, pp. 88-92, Mar 2018, doi: 10.1016/j.rmed.2018.02.003.

[35] H. Kumar, T. Kawai, and S. Akira, "Pathogen recognition by the innate immune system," Int Rev Immunol, vol. 30, no. 1, pp. 16-34, Feb 2011, doi: 10.3109/08830185.2010.529976.

[36] G. N. Barber, "STING: infection, inflammation and cancer,"

Nat Rev Immunol, vol. 15, no. 12, pp. 760-70, Dec 2015, doi: 10.1038/nri3921.

[37] J. Ahn and G. N. Barber, "STING signaling and host defense against microbial infection," Exp Mol Med, vol. 51, no. 12, pp. 1-10, Dec 11 2019, doi: 10.1038/s12276-019-0333-0.

[38] G. Dunphy et al., "Non-canonical Activation of the DNA Sensing Adaptor STING by ATM and IFI16 Mediates NF-kappaB Signaling after Nuclear DNA Damage," Mol Cell, vol. 71, no. 5, pp. 745-760 e5, Sep 6 2018, doi: 10.1016/j.molcel.2018.07.034.

[39] H. Maekawa et al., "Mitochondrial Damage Causes Inflammation via cGAS-STING Signaling in Acute Kidney Injury," Cell Rep, vol. 29, no. 5, pp. 1261-1273 e6, Oct 29 2019, doi: 10.1016/j.celrep.2019.09.050.

[40] C. Mohan and C. Putterman, "Genetics and pathogenesis of systemic lupus erythematosus and lupus nephritis," Nat Rev Nephrol, vol. 11, no. 6, pp. 329-41, Jun 2015, doi: 10.1038/nrneph.2015.33.

[41] S. Yung, D. Y. Yap, and T. M. Chan, "Recent advances in the understanding of renal inflammation and fibrosis in lupus nephritis," F1000Res, vol. 6, p. 874, 2017, doi: 10.12688/f1000research.10445.1.

[42] A. McLean-Tooke, I. Moore, and F. Lake, "Idiopathic and immune-related pulmonary fibrosis: diagnostic and therapeutic

challenges," Clin Transl Immunology, vol. 8, no. 11, p. e1086, 2019, doi: 10.1002/cti2.1086.

[43] J. W. Schoggins and G. Randall, "Lipids in innate antiviral defense," Cell Host Microbe, vol. 14, no. 4, pp. 379–85, Oct 16 2013, doi: 10.1016/j.chom.2013.09.010.

[44] P. Saas, A. Varin, S. Perruche, and A. Ceroi, "Recent insights into the implications of metabolism in plasmacytoid dendritic cell innate functions: Potential ways to control these functions," F1000Res, vol. 6, p. 456, 2017, doi: 10.12688/f1000research.11332.2.

[45] Y. Xiang, J. J. Tang, W. Tao, X. Cao, B. L. Song, and J. Zhong, "Identification of Cholesterol 25–Hydroxylase as a Novel Host Restriction Factor and a Part of the Primary Innate Immune Responses against Hepatitis C Virus Infection," J Virol, vol. 89, no. 13, pp. 6805–16, Jul 2015, doi: 10.1128/JVI.00587–15.

[46] D. Wu et al., "Type 1 Interferons Induce Changes in Core Metabolism that Are Critical for Immune Function," Immunity, vol. 44, no. 6, pp. 1325–36, Jun 21 2016, doi: 10.1016/j.immuni.2016.06.006.

[47] R. Billharz et al., "The NS1 protein of the 1918 pandemic influenza virus blocks host interferon and lipid metabolism pathways," J Virol, vol. 83, no. 20, pp. 10557–70, Oct 2009, doi: 10.1128/JVI.00330–09.

[48] J. C. Sun and L. L. Lanier, "NK cell development, homeostasis and function: parallels with CD8(+) T cells," Nat Rev Immunol, vol. 11, no. 10, pp. 645-57, Aug 26 2011, doi: 10.1038/nri3044.

[49] J. H. Kim, H. Y. Kim, S. Kim, J. H. Chung, W. S. Park, and D. H. Chung, "Natural killer T (NKT) cells attenuate bleomycin-induced pulmonary fibrosis by producing interferon-gamma," Am J Pathol, vol. 167, no. 5, pp. 1231-41, Nov 2005, doi: 10.1016/s0002-9440(10)61211-4.

[50] T. Y. Brodeur, T. E. Robidoux, J. S. Weinstein, J. Craft, S. L. Swain, and A. Marshak-Rothstein, "IL-21 Promotes Pulmonary Fibrosis through the Induction of Profibrotic CD8+ T Cells," J Immunol, vol. 195, no. 11, pp. 5251-60, Dec 1 2015, doi: 10.4049/jimmunol.1500777.

[51] O. Desai, J. Winkler, M. Minasyan, and E. L. Herzog, "The Role of Immune and Inflammatory Cells in Idiopathic Pulmonary Fibrosis," Front Med (Lausanne), vol. 5, p. 43, 2018, doi: 10.3389/fmed.2018.00043.

Abstract

특발성 폐섬유 질환 (IPF)은 간질성 폐질환 중 가장 흔하게 나타나는 질병으로 그 원인은 정확히 알려져 있지 않으며 지속적인 폐 섬유화를 일으킨다. IPF 환자는 호흡기 박테리아 감염에 취약하고 감염 시 폐섬유 증상을 악화시키지만 바이러스 감염에서는 무증상이거나 질병을 악화시키는 것과 무관하게 나타난다. 상피세포에서 나타나는 섬유화와 제1형 인터페론 (IFN-I)의 발현이 연관이 있는 것을 참조하여 실험자는 항바이러스 기전과 관련이 있는 면역계의 IFN-I이 IPF 환경에서 증가하여 IPF 이후 일어나는 바이러스 감염에 저항성을 부여하였을 것이라 가설을 세웠다. 우리의 연구는 bleomycin (BLM)으로 폐섬유화를 일으킨 마우스에서 IFN-I 의존적으로 인플루엔자 바이러스 감염에 저항성이 나타나는 것을 밝혔다. 증가한 IFN-I 은 BLM 처리 후 활성화된 STING/TBK1/IRF3 신호경로와 사멸시킴으로써 감소한 항바이러스 효과를 보여준 증가한 형질세포양 수지상 세포 (pDC)과 연관이 있는 것으로 보았다. 따라서 실험자는 BLM 유래 폐섬유 질환 동물 모델을 활용한 실험을 통해 IPF 환자에서 나타나는 바이러스 감염의 무증상은 STING/TBK1/IRF3 신호경로 활성화와 유입된 pDC 에 의한 IFN-I 발현 증가와 연관이 있을 것이라는 아이디어를 제시한다.